

Dimensional trend in CePt_2In_7 , Ce-115 compounds, and CeIn_3

Munehisa Matsumoto¹, Myung Joon Han², Junya Otsuki³, Sergey Yu. Savrasov¹

¹*Department of Physics, University of California, Davis, California 95616, USA*

²*Department of Physics, Columbia University, 538 West 120th Street, New York, New York 10027, USA*

³*Department of Physics, Tohoku University, Sendai 980-8578, Japan*

(Dated: December 30, 2018)

We present realistic Kondo-lattice simulation results for the recently-discovered heavy-fermion antiferromagnet CePt_2In_7 comparing with its three-dimensional counterpart CeIn_3 and the less two-dimensional ones, Ce-115's. We find that the distance to the magnetic quantum critical point is the largest for CeIn_3 and the smallest for Ce-115's, and CePt_2In_7 falls in between. We argue that the trend in quasi-two-dimensional materials stems from the frequency dependence of the hybridization between Cerium $4f$ -electrons and the conduction bands.

PACS numbers: 71.27.+a, 74.10.+v, 75.40.Mg

Recently-discovered CePt_2In_7 [1, 2] has provided a new approach toward the two-dimensional (2D) limit in CeIn_3 -derived heavy-fermion material family, among which Ce-115 materials have been discussed intensively in the past decade. In the hot debates on 115's, the possible scaling of the superconducting transition temperature T_c to c/a , where a and c are the lattice constants of the tetragonal crystal structure, has been discussed [3, 4] and there has been a hope to raise T_c by making a more 2D-like material. In this context $c/a = 4.694$ (if c should be taken to be the interlayer distance between Cerium planes, the scaling parameter should be taken to be 2.347) in CePt_2In_7 [2] looks promising as compared to the typical values of $c/a \sim 1.6$ in Ce-115's where the highest T_c 's have been found among Cerium heavy-fermion compounds [5–7].

Theoretically, the superconductivity (SC) with high T_c 's in strongly-correlated materials has been discussed to be mediated by magnetic fluctuations [8] and the possible mechanism for SC seems to be intimately related to the nearby magnetic quantum critical point (QCP) [9]. An empirical material-designing principle to get high T_c would be to make it as close as to QCP and it is desirable for a given possibly high- T_c material to know how close it is located to QCP. The robustness of the magnetic pairing has been discussed considering the spatial dimensional effects [10], stressing the stronger robustness in the more 2D-like systems even though care must be taken regarding the details of the electronic structure. Thus we are motivated to address QCP in CePt_2In_7 fully taking into account its electronic structure and see the trend among the related materials, namely, CeIn_3 with $c/a = 1$ and Ce-115's with slightly larger $c/a \simeq 1.6$, to see if any microscopic origin of c/a -scaling of T_c could be traced quantitatively to QCP. In the present work we predict the QCP's for all of these materials to elucidate where exactly CePt_2In_7 is located in the neighborhood of QCP.

Recent experiments on CePt_2In_7 [11] have shown that this material is an ideal Kondo lattice with commensu-

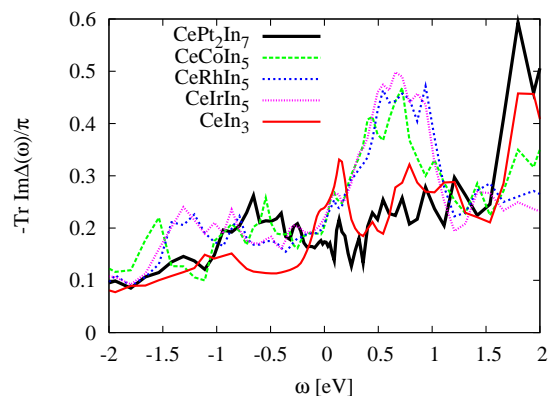


FIG. 1: (Color online) Hybridization function calculated by local density approximation (LDA) with Hubbard-I approximation for CePt_2In_7 , Ce-115's and CeIn_3 using the code described in Ref. [16]. The trace in the vertical axis quantity is taken over 14 orbitals of the $4f$ -orbital of Cerium.

rate antiferromagnetism. It can be a good target for realistic Kondo lattice simulations [12] for which it has been shown that the description works fine in the Kondo limit, meaning that local f -level position, ϵ_f , measured from the Fermi level should be negative and large, $U + \epsilon_f$ should be positive and large with U being the on-site Coulomb repulsion energy, and at the same time hybridization V^2 should not be too big. When the valence fluctuations start to dominate the Kondo lattice simulations does not work and we have to go back to the lattice simulations based on the Anderson impurity problem [13], which would increase the computational cost. It has been discussed that Ce-115's, especially CeRhIn_5 and CeIrIn_5 , have well localized electrons [14] and we expect that the comparison between CePt_2In_7 , $\text{CeRhIn}_5/\text{CeIrIn}_5$, and CeIn_3 in our simulations would make sense, while CeCoIn_5 might have to be looked at with some extra care.

We define our realistic Kondo lattice Hamiltonian starting with the first-principles electronic-structure cal-

calculation for the Cerium heavy fermion materials. The local density approximation (LDA) for delocalized s -, p -, and d -conduction electrons combined with the Hubbard-I approximation [15] for localized f -electrons gives the frequency-dependent hybridization function, $-\Im\Delta(\omega)/\pi$, between the conduction electrons and the localized $4f$ -electrons as shown in Fig. 1. A part of the trend is already seen at this stage: we find that the hybridization around the Fermi level, which is most relevant for Kondo screening [17], is the strongest for CeIn₃ and the weakest for CePt₂In₇, and Ce-115's comes in between. This is in line with the relevance of the off-plane hybridization that has been discussed for CeIrIn₅ [18]. Thus obtained data reflects the high-energy physics of the given material and then we obtain our low-energy Hamiltonian via the Schrieffer-Wolff transformation [19] implemented in a realistic way [12]. The Kondo coupling $J_K = V^2[1/|\epsilon_f| + 1/(U_{\text{eff}} + \epsilon_f)]$ incorporates the virtual hopping process $f^1 \rightarrow f^0$ in the first term and in the second term another virtual process $f^1 \rightarrow f^2$ with $U_{\text{eff}} = U - J_{\text{Hund}} \sim 4$ [eV] being the effective on-site Coulomb energy in the f^2 multiplet in the Ce atom including the effective Hund coupling $J_{\text{Hund}} \sim 1$ [eV]. The hybridization V^2 is taken to be $\int_{-\infty}^D d\omega [-\Im\Delta(\omega)/\pi]$, to take care of the normalization of the density of states of our conduction electrons with keeping the value of a relevant quantity in Kondo physics, $J_K\rho(\omega)$, where $\rho(\omega)$ is the conduction electron density of states, to the given realistic value. Note that the conduction band cutoff D matters in the definition of J_K . Although $-\Im\Delta(\omega)/\pi$ is a decaying function of $\omega \gg 0$, it does not fall off sufficiently fast due to numerically imperfect projection onto f -states. Thus the cutoff D is implemented to be equal to the on-site Coulomb energy $D = U = 5$ [eV]. The relevant parameters and the outputs of LDA for the Cerium compounds of our present interest is summarized in Table I. We note that our calculated values of ϵ_f for Ce-115's are not exactly consistent with the photoemission data in the literature [14, 26]. However both of the calculated values and experimental ones indicate that all of the materials are deep in the Kondo regime. The spin-orbit splittings are set to be 0.3 [eV] for all of the materials. The structural parameters to be plugged into LDA are taken from experiments referring to Ref. [25].

Now we describe how we solve the realistic Kondo lattice model (KLM) that we have defined from $-\Im\Delta(\omega)/\pi$ in Fig. 1 and Table I. We use dynamical mean-field theory (DMFT) [27, 28] that is formulated on a local f -electron basis [29] which enables us to reach low temperature region with a modest computational cost and address the QCP in a semi-quantitative way utilizing state-of-the-art continuous-time quantum Monte Carlo (CT-QMC) impurity solver [30–33]. We plug-in the realistic crystal-field and spin-orbit splittings as given in Table I in the local $4f$ -level in the impurity problem. Thus our solutions are numerically exact up to the approximation

TABLE I: The parameters for the investigated materials. The first two columns are LDA + Hubbard-I results for the local f -level position ϵ_f and the value of the hybridization function on the Fermi level. The final column shows the crystal-field splittings in the tetragonal structure.

	ϵ_f [eV]	$-\text{Tr}\Im\Delta(0)/\pi$ [eV]	Δ_1 and Δ_2 [meV]
2D CePt ₂ In ₇	-1.81	0.174	8.6, 12.9 ^a
CeCoIn ₅	-1.97	0.205	6.8, 25 ^b
CeRhIn ₅	-1.90	0.209	5.9, 28.5 ^c
CeIrIn ₅	-1.95	0.220	5.26, 25.875 ^c
3D CeIn ₃	-1.72	0.239	12 ^d

^a = 100 [K] and 150[K], a rough estimate [20].

^b Ref. [21, 22]. Another crystal-field scheme in Ref. [23] gives essentially the same results.

^c Ref. [24]. The latest crystal-field schemes in Ref. [21] give the values close to these.

^d Ref. [25]. This materials has the cubic structure which brings $\Delta_1 = \Delta_2$.

of DMFT. We look at the magnetic phase transition as a function of temperature and restore the Doniach phase diagram [34] by varying the Kondo coupling J_K for a given material. Thus a magnetic QCP is found on a realistic Doniach phase diagram spanned by the Kondo coupling and temperature, and the realistic data point for the given material is picked up for the realistic value of $U = 5$ [eV] and $J_{\text{Hund}} = 1$ [eV] to estimate its distance to QCP.

Now we show how we determine the QCP of CePt₂In₇. The calculated temperature dependence of the inverse of the staggered magnetic susceptibility, $1/\chi(\pi)$, for CePt₂In₇ is shown in Fig. 2. Here we have employed random dispersion approximation [35] to estimate the two-particle Green's function by decoupling, which would enhance our transition temperatures on top of DMFT as will be seen below. Being consistent with Doniach's picture [34] where the winner of the competition between the magnetic-ordering energy scale $\propto J_K^2\rho$ and the Kondo-screening energy scale $\propto \exp[-1/(J_K\rho)]$ interchanges at some finite J_K , it is seen that small J_K 's give a diverging $\chi(\pi)$ at a finite Néel temperature T_N while large J_K 's give a saturating $\chi(\pi)$ at low temperatures, and some value of J_K in between gives the quantum critical point where T_N vanishes. The Néel temperatures for smaller J_K 's are determined by linear extrapolation of $1/\chi(\pi)$ to the lowest temperature region and thus obtained T_N is plotted against the Kondo coupling in Fig. 3 in a format of restored Doniach phase diagram. Here we note that we just identified what we call QCP by a parameter segment where the finite Néel temperature seems to have vanished, and there is always a possibility that in some smaller parameter segments there is actually a coexistence region. There is also a possibility numerically for a

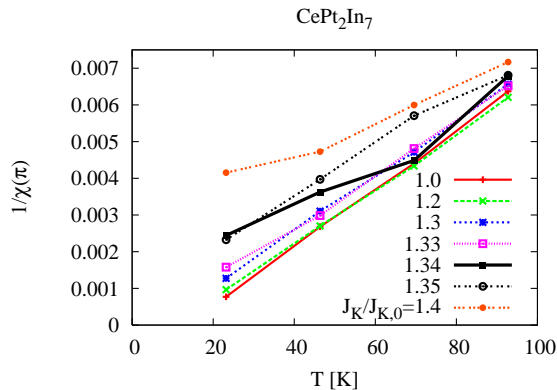


FIG. 2: (Color online) Temperature dependence of the inverse of the staggered susceptibility in the realistic Kondo lattice models for CePt_2In_7 by which we identify that the phase boundary is located in $1.33J_{K,0} < J_K < 1.34J_{K,0}$, where $J_{K,0}$ is the Kondo coupling which corresponds to $U = 5$ [eV] and $J_{\text{Hund}} = 0$.

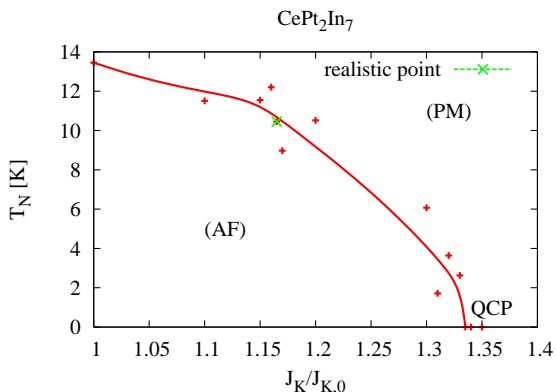


FIG. 3: (Color online) Restored realistic Doniach phase diagram for CePt_2In_7 from the data in Fig. 2. AF is the antiferromagnetic phase and PM is the paramagnetic phase. The line is a guide to the eye.

first-order phase transition where the Néel temperature actually jumps from a finite value to zero at a certain point of J_K . We leave the exact characterization of what we also call QCP here for future investigations and for the moment we would be satisfied with that it looks like QCP practically in most cases with a very small jump numerically, if any.

For CePt_2In_7 , the realistic data point is at $J_K = 1.165J_{K,0}$, which corresponds to $U = 5$ [eV] and $J_{\text{Hund}} = 1$ [eV], gives the Néel temperature $T_N \simeq 10$ [K] which is larger than the experimental result $T_N = 4.5$ [K] [11] due to our mean-field argument with DMFT and the random dispersion approximation [35] which becomes exact on a lattice with perfect nesting. The same analyses are applied to the other materials to give the Néel temperature $T_N = 19$ [K] for CeIn_3 , 15 [K] for CeRhIn_5 , and 14 [K] for CeCoIn_5 . Again the experimental values ($T_N = 10.2$ [K]

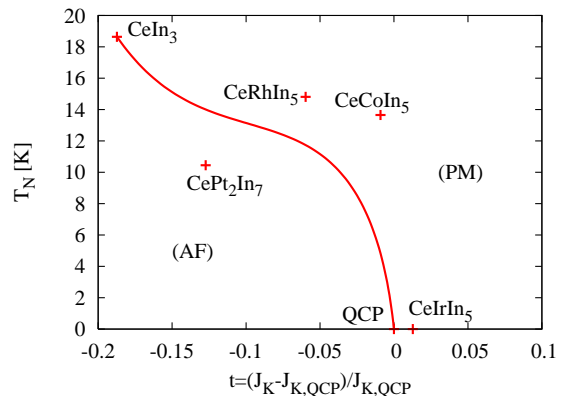


FIG. 4: (Color online) Realistic Doniach phase diagram for CePt_2In_7 , and Ce-115's together with their parent compound, CeIn_3 with the horizontal axis rescaled to measure the distance to the magnetic QCP. The line is a guide to the eye.

for CeIn_3 , 3.8 [K] for CeRhIn_5 [5, 25]) comes below these results. The data for CeCoIn_5 is not consistent with the experimental fact that CeCoIn_5 is a non-magnetic heavy fermion material [6]. However the arrangement of the materials around QCP reveals that the apparent finite T_N actually comes from being in an immediate proximity to QCP as shown in Fig. 4. We use a rescaled Kondo coupling on the horizontal axis in terms of its value right on the QCP, $t \equiv (J_K - J_{K|QCP})/J_{K|QCP}$, to remove a problem with the Doniach phase diagram that each material has its own energy scales.

Now we inspect the distance to the QCP of CePt_2In_7 referring to those of Ce-115's and CeIn_3 . The cubic parent material CeIn_3 is seen to be most separated from QCP and Ce-115's are found to be concentrated in the neighborhood to QCP, with CeRhIn_5 on the magnetic side and CeIrIn_5 on the non-magnetic side. Our numerical resolution is not sufficient to locate CeCoIn_5 in its correct non-magnetic side, but it is clear that it sufficiently works to estimate the extreme closeness to QCP of Ce-115's. We note that our calculation scheme might not be as good for CeCoIn_5 as for the others due to the possibly stronger effects of valence fluctuations in this material. It is seen that when we try to reach the quantum critical point (QCP) from CeIn_3 in the three-dimensional limit, CePt_2In_7 is located in the midway toward Ce-115's which are located closest to the QCP. Seen from QCP, CeIn_3 is already close enough to enable the pressure-driven superconductivity [36] and CePt_2In_7 would also have one. Making a material more 2D indeed helps it to come closer to QCP, which is reasonable in the general context that the lower spatial dimensionality would suppress the magnetic long-range order. However within the 2D-side, the trend among CePt_2In_7 and Ce-115's is somewhat non-monotonic. The possible reason is seen in Fig. 1, where a dip around the Fermi level is seen for CePt_2In_7 which would help to drive it to the magnetic side with the re-

duced Kondo screening. On top of the spatial dimensionality, the frequency dependence of the hybridization seems to introduce the nontrivial trend in this way.

Here we note that precisely speaking we are discussing in the infinite-dimensional limit with the DMFT, but at least a semi-quantitative trend of T_N would be satisfactorily addressed. We also note that in the literature the importance of momentum dependence of the hybridization has been stressed [18, 37, 38] which we have neglected. What we have seen is that the energy dependence seems to be sufficient at least to capture the trend in the distance to QCP, thus for the prediction of magnetically-mediated superconductivity with a possible high T_c .

In order to reach QCP, it would be interesting to have a material analogous to CePt_2In_7 but without a big dip in the hybridization around the Fermi level. For that, the following possible ways for the material designing could help: 1) electronic carrier doping, 2) ascending T in the periodic table for CeT_2In_7 to enhance the hybridization, and 3) shifting T to the left- or the right-hand side on the periodic table to lift the dip off the Fermi level to enable the stronger Kondo coupling to drive the material toward the QCP side.

Finally we discuss the degree of the delocalization of f -electrons by looking at their contribution to the Fermi surface of the conduction electrons in our realistic Kondo lattice description for each material. Even if we have only localized f -electrons in our Hamiltonian, they contribute to the formation of the large Fermi surface via the hybridization and in this sense they can be delocalized [39]. We follow the procedure used in Ref. [40]. From our simulations for a give material at a fixed temperature, we get the conduction-electron self energy $\Sigma(i\omega_n)$ and then track the temperature dependence of the real part of it at $i\omega_n = 0$ to look at the shift of the Fermi level. Here $\omega_n = (2n + 1)\pi T$ is the fermion Matsubara frequency. The result is plotted in Fig. 5. It is seen that CePt_2In_7 has the most localized f -electrons down to the temperature range of 20 [K] among these materials while the 115's have the strongest delocalization. CeIn_3 falls in between. We note that the trend in the f -electron delocalization does not exactly follow that in the hybridization strength right on the Fermi level seen in Fig. 1 and it is the outcome of the frequency dependence of the hybridization that we have taken into account in our realistic Kondo lattice simulations.

To conclude, we have predicted the QCP of CePt_2In_7 and discussed the possible strategy to have the higher T_c in the related material family within our realistic Kondo lattice description which has been shown to predict the properties of Ce-115's and their parent material CeIn_3 semi-quantitatively. Our method's predictability of magnetic QCP would further provide the material designing principle toward more high- T_c materials in the upcoming material exploration.

MM thanks Nick Curro, Owen Dix, Ruanchen Dong,

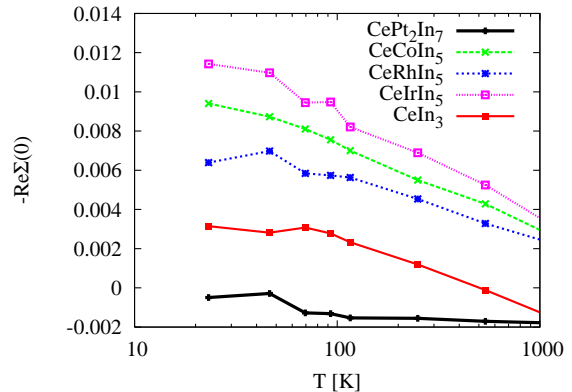


FIG. 5: (Color online) Temperature dependence of the real part of the conduction-electron self-energy for CePt_2In_7 , Cerium-115's and CeIn_3 .

Ravindra Nanguneri, Hiroaki Shishido for discussions. The present numerical calculations has been done on “Chinook” in Pacific Northwest National Laboratory, on “Ranger” in Texas Advanced Computing Center at the University of Texas at Austin under the TeraGrid grant DMR090100, and on a local PC cluster machine in UC Davis. This work was supported by DOE SciDAC Grant No. SE-FC02-06ER25793 and by DOE NEUP Contract No. 00088708.

-
- [1] E. D. Bauer *et al.*, APS March meeting 2010, A38.00004.
 - [2] Zh. M. Kurenbaeva *et al.*, *Intermetallics* **16**, 979 (2008).
 - [3] E. D. Bauer *et al.*, *Phys. Rev. Lett.* **93**, 147005 (2004).
 - [4] Purely geometrical effect in the c/a scaling in CeIrIn_5 has been carefully discussed in O. M. Dix. *et al.* *Phys. Rev. Lett.* **102**, 197001 (2009).
 - [5] H. Hegger *et al.*, *Phys. Rev. Lett.* **84**, 4986 (2000).
 - [6] C. Petrovic *et al.*, *J. Phys: Condens. Matter*, **13**, L337 (2001).
 - [7] C. Petrovic *et al.*, *Europhys. Lett.* **53**, 354 (2001).
 - [8] P. Monthoux, D. Pines, and G. G. Lonzarich, *Nature* **450**, 1177 (2007).
 - [9] S. Sachdev, *Quantum Phase Transitions*, Cambridge (1999).
 - [10] P. Monthoux and G. G. Lonzarich, *Phys. Rev. B* **63**, 054529 (2001); **66**, 224504 (2002).
 - [11] N. apRoberts-Warren *et al.*, arXiv:1002.3204.
 - [12] M. Matsumoto, M. J. Han, J. Otsuki, S. Y. Savrasov, *Phys. Rev. Lett.* **103**, 096403 (2009).
 - [13] P. W. Anderson, *Phys. Rev.* **124**, 41 (1961).
 - [14] S.-I. Fujimori *et al.*, *Phys. Rev. B* **73**, 224517 (2006); *Phys. Rev. B* **67**, 144507 (2003).
 - [15] J. Hubbard. *Proc. R. Soc. London, Ser. A* **276**, 238 (1963); **277**, 237 (1964); **281**, 401 (1964).
 - [16] S. Y. Savrasov, *Phys. Rev. B* **54**, 16470 (1996).
 - [17] S. Burdin, A. Georges, and D. R. Grempel, *Phys. Rev. Lett.* **85**, 1048 (2000).
 - [18] J. H. Shim, K. Haule, and G. Kotliar, *Science* **318**, 1615 (2007).

- [19] J. R. Schrieffer and P. A. Wolff, Phys. Rev. **149**, 491 (1966)
- [20] N. J. Curro, private communications.
- [21] T. Willers *et al.*, arXiv:1003.0300.
- [22] A. D. Christianson *et al.*, Phys. Rev. B **70**, 134505 (2004) and Hiroaki Shishido (private communications).
- [23] S. Nakatsuji *et al.*, Phys. Rev. Lett. **89**, 106402 (2002).
- [24] S. Takeuchi *et al.*, J. Phys. Soc. Jpn. **70**, 877 (2001).
- [25] C. Pfleiderer, Rev. Mod. Phys. **81**, 1551 (2009).
- [26] A. Koitzsch *et al.*, Phys. Rev. B **79**, 075104 (2009); Phys. Rev. B **77**, 155128 (2008).
- [27] A. Georges, G. Kotliar *et al.*, Rev. Mod. Phys. **68**, 13 (1996).
- [28] G. Kotliar, S. Savrasov *et al.*, Rev. Mod. Phys. **78**, 865 (2006).
- [29] J. Otsuki, H. Kusunose, and Y. Kuramoto, J. Phys. Soc. Jpn. **78**, 014702 (2009).
- [30] A. N. Rubtsov, V. V. Savkin, and A. I. Lichtenstein, Phys. Rev. B **72**, 035122 (2005).
- [31] P. Werner, A. Comanac, L. de' Medici, M. Troyer, and A. J. Millis, Phys. Rev. Lett. **97**, 076405 (2006); P. Werner and A. J. Millis, Phys. Rev. B **74**, 155107 (2006).
- [32] K. Haule, Phys. Rev. B **75**, 155113 (2007).
- [33] J. Otsuki, H. Kusunose, P. Werner and Y. Kuramoto, J. Phys. Soc. Jpn. **76**, 114707 (2007).
- [34] S. Doniach, Physica B **91**, 231 (1977).
- [35] F. Gebhard, *The Mott Metal-Insulator Transition*, Springer Tracts in Modern Physics Vol. 137 (Springer-Verlag, Berlin, 1997).
- [36] N. D. Mathur *et al.*, Nature **394**, 39 (1998).
- [37] K. S. Burch *et al.*, Phys. Rev. B **75**, 054523 (2007).
- [38] K. Haule, C.-H. Yee, and K. Kim, arXiv:0907.0195.
- [39] R. M. Martin, Phys. Rev. Lett. **48**, 362 (1982).
- [40] J. Otsuki, H. Kusunose, and Y. Kuramoto, Phys. Rev. Lett. **102**, 017202 (2009).